

UC Irvine

UC Irvine Previously Published Works

Title

KCNK2: reversible conversion of a hippocampal potassium leak into a voltage-dependent channel

Permalink

<https://escholarship.org/uc/item/4ft0c4xw>

Journal

Nature Neuroscience, 4(5)

ISSN

1097-6256

Authors

Bockenhauer, Detlef

Zilberberg, Noam

Goldstein, SAN

Publication Date

2001-05-01

DOI

10.1038/87434

Copyright Information

This work is made available under the terms of a Creative Commons Attribution License, available at <https://creativecommons.org/licenses/by/4.0/>

Peer reviewed

# KCNK2: reversible conversion of a hippocampal potassium leak into a voltage-dependent channel

Detlef Bockenhauer, Noam Zilberberg and S. A. N. Goldstein

Departments of Pediatrics and Cellular and Molecular Physiology, Boyer Center for Molecular Medicine, Yale University School of Medicine, 295 Congress Avenue, New Haven, Connecticut 06536, USA

Correspondence should be addressed to S.A.N.G. (steve.goldstein@yale.edu)

Potassium leak channels are essential to neurophysiological function. Leaks suppress excitability through maintenance of resting membrane potential below the threshold for action potential firing. Conversely, voltage-dependent potassium channels permit excitation because they do not interfere with rise to threshold, and they actively promote recovery and rapid re-firing. Previously attributed to distinct transport pathways, we demonstrate here that phosphorylation of single, native hippocampal and cloned KCNK2 potassium channels produces reversible interconversion between leak and voltage-dependent phenotypes. The findings reveal a pathway for dynamic regulation of excitability.

Potassium leak currents have been recognized as essential to neuromuscular function for over fifty years<sup>1-5</sup>. Also called resting (or background) conductances, their existence as unique molecular transport entities was questioned even as they were attributed key roles in sympathetic ganglia, invertebrate axons, vertebrate myelinated axons and cardiac myocytes<sup>6-11</sup>. Operating under control of agents as disparate as serotonin, cyclic nucleotides, molecular oxygen and  $\gamma$ -aminobutyric acid, potassium leak establishes and maintains a hyperpolarized resting membrane potential that suppresses excitatory responses, whereas inhibition of the leak produces a permissive state<sup>11-14</sup>. Native leaks have defied coherent description, perhaps because they seem to be invariant, and are easily camouflaged by time-dependent processes. However, cloning of TOK1 from *Saccharomyces cerevisiae*<sup>15</sup>, KCNK0 from *Drosophila melanogaster*<sup>16</sup> and, to date, twelve mammalian KCNK genes for 2 P domain potassium-selective leak channels, has affirmed that these currents are carried by dedicated pathways amenable to detailed study<sup>17</sup>.

The human KCNK2 gene encodes a 426-residue KCNK2 channel subunit with two pore-forming P domains and four transmembrane segments (a 2P/4TM topology), and gains high expression in central nervous system tissues, especially the hippocampus<sup>18</sup>. Referred to as TPKC1 (ref. 18) or TREK1 (ref. 19), and now KCNK2 for clarity, the channel has been implicated in neural responses to temperature, arachadonic acid, mechanical stretch and volatile anesthetics<sup>19-21</sup>. Here we sought to understand the discrepant attributes accorded KCNK2 channels<sup>18-23</sup>. We report that the single canonical site in KCNK2 for protein kinase A (PKA) phosphorylation, previously shown to mediate temperature sensitivity<sup>20</sup>, controls not only the amount of channel activity, but its fundamental response to voltage.

## RESULTS

### Native KCNK2 channels: phenotypic interconversion

To allow direct comparison of native and cloned channels, rat KCNK2 was cloned and found to share 95% identity with the human gene at the amino acid level, including a PKA consensus site with serine at position 348 (see Methods). Rat hippocampal cells carrying a temperature-sensitive simian large tumor antigen gene<sup>24</sup> expressed KCNK2 messenger RNA only when driven to differentiate (Fig. 1a). Thus, reverse transcription generated no signal from undifferentiated cells but a band of the expected size for KCNK2 with RNA isolated from cells induced to mature to primary neurons. Accordingly, KCNK2-like channels were not observed in small on-cell patches with undifferentiated cells ( $n = 46$ ), but were apparent with mature cells in 5 of 20 patches having only one to three channels. (Seventeen other patches had too many channels to evaluate, and 111 were quiet; to reduce activity of other native channels, long pre-pulse depolarizations were used to silence channels subject to inactivation, and pipette and bath solutions contained 1 mM magnesium and no sodium or calcium.) When native KCNK2-like channels were excised from cells in inside-out mode and treated with the catalytic sub-unit of PKA (20 U/ml) and ATP (1 mM), they showed a decrease in activity at  $-60$  mV

that was reversed by exposure to alkaline phosphatase (AP, 20 U/ml; Fig. 1b).

Evaluation of single native channels at a variety of potentials revealed that enzyme-induced changes in activity at  $-60$  mV resulted from a unique regulatory alteration in channel phenotype. After AP treatment, the channels opened frequently, in a voltage-insensitive fashion: at  $100$  mV, open probability ( $P_{O100}$ ) was  $0.80 \pm 0.08$  ( $n = 3$ ), which was steadily maintained from  $-100$  to  $100$  mV ( $P_{O-100}/P_{O100} = 0.93 \pm 0.10$ ,  $n = 3$ ; Fig. 1c, left). Conversely, treatment with PKA and ATP yielded channels with decreased activity ( $P_{O100} = 0.11 \pm 0.09$ ,  $n = 3$ ) that were  $\sim 100$ -fold more active at depolarized potentials ( $P_{O-100}/P_{O100} = 0.01 \pm 0.00$ ,  $n = 3$ ; Fig. 1c, right). These voltage-dependent changes in activity produced significant outward currents and limited inward currents despite symmetric potassium levels across the membrane. Three single native channels were thus reversibly interconverted by AP or PKA and ATP between two phenotypes: a voltage-insensitive open pore and a voltage-dependent outward rectifier

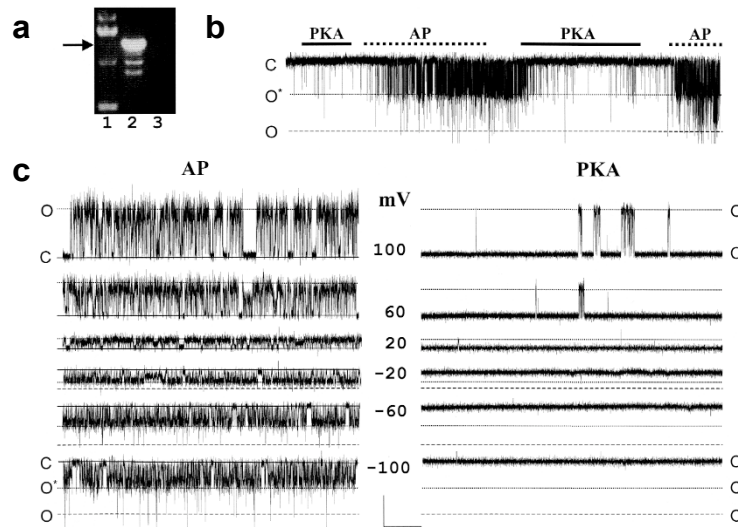


**Fig. 1.** Native KCNK2 leak pores are reversibly transformed into voltage-dependent channels by PKA-mediated phosphorylation. Recordings were taken in symmetric  $100$  mM KCl and  $1$  mM MgCl<sub>2</sub> solution. C, closed state (solid line); O\* and O, open states (dashed lines). In the presence of magnesium, channels show two open states at negative potentials. (a) Reverse transcription with KCNK2-specific primers demonstrates the presence of KCNK2 messenger RNA in a rat hippocampal cell line in the mature (lane 2) but not the undifferentiated state (lane 3). Markers (lane 1),  $0.5$ ,  $1$ ,  $1.5$  and  $2$  kb; arrow, size of expected product ( $1427$  bp). (b) A single native channel in inside-out patch mode shows decreased activity when treated with PKA and ATP and increased activity with AP at  $-60$  mV. Trace duration,  $7$  min. Sampled at  $1$  kHz, filtered at  $200$  Hz. Open levels O\* and O,  $-3.0$  and  $-6.7$  pA, respectively. (c) A single native channel at various voltages (as indicated) shows a high uniform  $P_o$  in the presence of AP (left panel) and voltage-dependent outward rectification after treatment with PKA and ATP (right panel). Scale bars,  $5$  pA and  $100$  ms; sampled at  $20$  kHz, filtered at  $2$  kHz. At  $100$  mV open level  $8.0$  pA and  $-100$  mV, O\* and O are  $-3.2$  and  $-8.1$  pA, respectively.

### Native and cloned KCNK2: biophysical equivalence

Several lines of evidence argued that the native channel under study was KCNK2. First, single native and cloned KCNK2 channels had the same primary slope conductance ( $85 \pm 2$  and  $84 \pm 1$  pS, respectively, in symmetrical  $100$  mM KCl from  $-20$  and  $100$  mV; Fig. 2a). Second, isotonic replacement of rubidium for potassium as charge carrier yielded a new primary slope conductance in both native and cloned KCNK2 channels ( $64 \pm 1.4$  and  $64 \pm 3.3$  pS, respectively) and similarly increased  $P_o$  (Fig. 2b). Third, magnesium at physiological concentration ( $1$  mM) similarly inhibited single native and cloned KCNK2 channels to produce two open states at hyperpolarized potentials, consistent with unblocked (O) and blocked current levels (O\*; Fig. 2c); thus, the amplitude of O\* was  $-3.4 \pm 0.9$  and  $-3.3 \pm 0.9$  pA at  $-60$  mV and  $2$  kHz for native and cloned channels, respectively (Figs. 1b, c and 2c), and half-maximal at  $-81 \pm 4$  mV (data not shown). Fourth, the effects of PKA and ATP or AP on native and cloned KCNK2 channel gating parameters were similar (Fig. 2d). Thus, dwell time in the principle open state (O\*) at  $-60$  mV was the same for the two channels and unchanged

by application of PKA and ATP or AP ( $1.90 \pm 0.05$  and  $2.00 \pm 0.05$  ms for native and cloned channels with AP, respectively,  $n = 3$ ). Furthermore, both channels demonstrated two closed states at  $-60$  mV. The briefer closure was unaffected by phosphorylation ( $0.50 \pm 0.10$  and  $0.50 \pm 0.05$  ms for native and cloned channels with AP, respectively,  $n = 3$ ) and was apparent in single channel records as ‘flickery’ transitions within open bursts. The longer closure had a mean dwell time of  $\sim 5$  ms in the presence of AP ( $5.0 \pm 0.4$  and  $6.1 \pm 1.0$  ms for native and cloned channels, respectively,  $n = 3$ ) and increased in frequency  $\sim 10$ -fold (from  $\sim 0.02$  to  $0.20$  of closures) and duration  $\sim 200$ -fold ( $1200 \pm 900$  and  $1700 \pm 2000$  ms for native and cloned channels,  $n = 3$ , respectively) after PKA and ATP treatment. This was reminiscent of kinase regulation of KCNK0, in which the frequency and duration of visits to a long closed state were altered; although, in that case, phosphorylation increased activity in a voltage-independent fashion<sup>25</sup>.

### **A direct effect via KCNK2 serine 348**

To investigate the mechanistic basis for these phenotypic inter-conversions, cloned human KCNK2 channels were studied further. Single wild-type channels showed expected changes in channel activity with enzyme exposure at  $-60$  mV (Fig. 3a). Thus, PKA and ATP decreased KCNK2 activity ( $P_{O100} = 0.18 \pm 0.15$ ,  $n = 2$ ) and yielded channels  $\sim 100$ -fold more active at depolarized voltages ( $P_{O-100}/P_{O100} = 0.03 \pm 0.04$ ,  $n = 2$ ), whereas AP increased channel activity ( $P_o = 0.68 \pm 0.03$ ,  $n = 2$ ) in a uniform fashion across a wide voltage range ( $P_{O-100}/P_{O100} = 0.90 \pm 0.10$ ,  $n = 2$ ). To determine if the enzymes were acting directly on KCNK2, serine 348 (in the PKA consensus site) was first changed to alanine (S348A) to mimic the non-phosphorylated state. Single S348A channels (Fig. 3b, left) were similar to AP-treated native or wild-type cloned channels, demonstrating a high, uniform  $P_o$  across the voltage range ( $P_{O100} = 0.53 \pm 0.08$ ,  $P_{O-100}/P_{O100} = 1.0 \pm 0.2$ ,  $n = 6$ ). Next, serine 348 was mutated to aspartate (S348D) to coarsely resemble KCNK2 in the phosphorylated state. Single S348D channels (Fig. 3b, right) recapitulated the effect of PKA and ATP on native and cloned wild-type channels, yielding voltage-dependent outward rectification ( $P_{O100} = 0.21 \pm 0.05$ ,  $P_{O-100}/P_{O100} = 0.02 \pm 0.02$ ,  $n = 6$ ). The function of S348A or S348D channels was not altered by application of either PKA and ATP or AP, consistent with regulation of wild-type channels by phosphorylation of serine 348 ( $n = 2$ ; Fig. 3c).

The idea that changes in KCNK2 phenotype were mediated directly by phosphorylation of serine 348 (rather than by involvement of other proteins<sup>26</sup>) was supported by study of channels altered to cysteine (S348C) and exposed to 2-sulfonatoethyl methanethiosulfonate (MTSES), a reagent that covalently modifies cysteine to leave a negatively charged sulfonatoethyl moiety. In unmodified form, S348C channels showed a voltage-insensitive  $P_o$  like S348A channels or wild-type channels treated with AP (data not shown). Whereas wild-type channels were insensitive (data not shown), S348C channels treated with 10 mM internal MTSES decreased in activity at  $-60$  mV (Fig. 3d), similarly to wild-type channels treated with PKA and ATP (Fig. 3a); the change was stable, despite reagent wash-out, until chemical reduction (Fig. 3d), consistent with covalent modification at position 348.

## **DISCUSSION**

Potassium channels control neuronal excitability through influence over the duration, frequency and amplitude of action potentials. Potassium channels that are active at rest inhibit depolarization toward firing threshold, and thus suppress excitation. Conversely, potassium channels activated at depolarized potentials do not interfere with rise to threshold, but do facilitate recovery and repetitive firing. Here we identified a pathway for regulation of neuronal excitability. Native hippocampal and cloned KCNK2 channels transform in a regulated and reversible fashion from potassium-selective leak conductances (open across the physiological voltage range) to strictly voltage-dependent channels.

### **Comparison to voltage effects on other channels**

Inwardly rectifying (Kir) channels contribute to potassium leak, stabilizing cells near the equilibrium reversal potential of potassium ( $E_K$ )<sup>27-30</sup>. Formed of subunits with one P domain and two transmembrane segments (1P/2TM), Kir channels pass small outward currents because of pore blockade by internal magnesium and polyamines; at potentials negative to  $E_K$ , large inward currents are passed upon relief from blockade. An analogous process, that is, pore occlusion by an external cation, cannot explain outward currents in KCNK2

channels, first, because the activation midpoint ( $V_{1/2}$ ) for S348D channels was insensitive to changes in  $E_K$ . Thus, in symmetric 100-mM potassium,  $V_{1/2}$  was  $10 \pm 7$  mV (predicted  $E_K \sim 0$  mV), whereas after isotonic replacement of 95 mM bath potassium for sodium,  $V_{1/2}$  was  $8 \pm 10$  mV (predicted  $E_K \sim -85$  mV; Fig. 4a). Moreover, whereas external magnesium did produce inhibition at negative voltages (Fig. 2c), both S348A and S348D channels were influenced equally (Fig. 4b). Finally, the  $V_{1/2}$  of S348D channels was also unaltered in the absence of added divalent cations (with EGTA), or when ultra-pure potassium was used to reduce heavy metal contamination (data not shown).

TOK1 has a predicted 2P/8TM topology, and thus shares with KCNK2 a two-P-domain subunit structure; however, TOK1 functions distinctly<sup>15</sup>. Reminiscent of a Kir channel (but with reciprocal rectification properties), this target for viral K1 Killer toxin<sup>31</sup> is a non-voltage-gated outward rectifier that passes significant outward potassium currents at potentials positive to  $E_K$  by a mechanism that seems to involve both conformational changes of the protein and ion occupancy of the pore<sup>15,32–35</sup>.

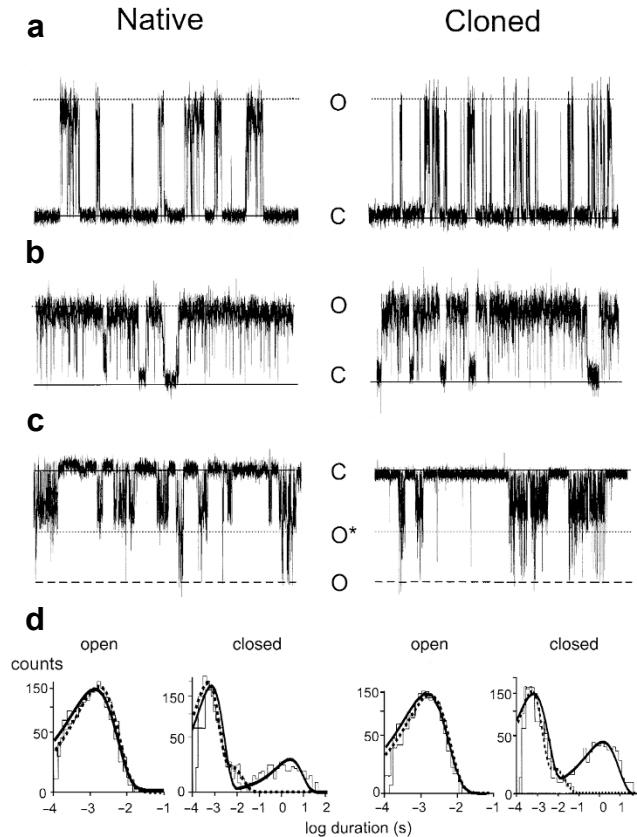


**Fig. 2.** Native and cloned KCNK2 channels show the same biophysical properties. Patches were excised in inside-out mode from differentiated hippocampal cells or oocytes expressing cloned KCNK2, and were studied with symmetric 100 mM KCl unless otherwise indicated. Traces of 1 s are shown; sampled at 20 kHz, filtered at 2 kHz. Channel state designations as in Fig. 1. (a) Native and cloned channels have the same major unitary conductance and appearance. Shown at 100 mV; principle conductance values are in text. (b) Native and cloned channels have the same current level and appearance with rubidium as charge carrier. In this case, bath solution was replaced isotonicly by 100 mM RbCl. Shown at 100 mV; dashed line open level, 5.4 pA. With 1 mM MgCl<sub>2</sub> added, native and cloned channels show two open state levels at negative voltages. Shown at -60 mV, lines for O\* and O are indicated at -3.0 and -6.7 pA, respectively. (d) Dwell-time histograms of native and cloned KCNK2 channels at -60 mV reveal one open and two closed states. One open state is apparent in the presence of AP (dashed line) or PKA and ATP (solid line) with mean duration  $2.3 \pm 0.1$  ms (native) and  $2.1 \pm 0.2$  ms (cloned) with PKA and ATP ( $n = 3$ ); values for AP are in the text. Histograms suggest two closed states for both native and cloned channels in the presence of AP (dashed line) or PKA and ATP (solid line); the briefer closure was unaffected by phosphorylation, and was  $0.7 \pm 0.3$  ms (native) and  $0.6 \pm 0.3$  ms (cloned) with PKA and ATP ( $n = 3$ ); values for AP are in the text. The longer closure had a mean dwell time of  $\sim 5$  ms with AP and increased in frequency and duration with PKA and ATP treatment (values in text). Closed and open-time duration were determined using half-amplitude threshold detection<sup>46</sup>. Dwell-time distributions were plotted on a logarithmic time axis with a square-root vertical axis to best discern event populations; histograms were fitted with TacFit software (Bruyton, Seattle, Washington) using a sums of exponential probability density function and maximum likelihood method.

Classical voltage-gated potassium channel (Kv) subunits, in an  $E_K$ -insensitive fashion, are quiet at rest and show increased  $P_o$  with membrane depolarization; this is similar to KCNK2 when it functions in a voltage-dependent manner (Fig. 4a). Kv channels are formed by subunits with a 1P/6TM topology, and carry a special fourth span (S4) with positively charged residues at every third or fourth position that acts as a voltage sensor and moves in response to changes in membrane potential. KCNK2 has no charges in its predicted transmembrane segments to suggest it uses a similar type of voltage sensor. The voltage dependence of S348D KCNK2 activation (estimated roughly from a fit to the  $P_o$ -voltage relationship, Fig. 4a) suggests a net movement of  $\sim 2.5$  elemental charges across the field, compared to  $\sim 4-6$  elemental charges (determined by the same method) for the classical voltage-gated potassium channel Shaker.

Phenotypic conversion of KCNK2 recalls the highly regulated transition of voltage-gated calcium channels between ‘willing’ and ‘reluctant’ states, which differ significantly in their voltage dependence for activation. (These channels are formed by large proteins resembling four 1P/6TM units linked in tandem, and bear four S4 voltage sensors<sup>38,39</sup>.) In this analogy, dephosphorylated KCNK2 is still voltage dependent, but has a hyperpolarized  $V_{1/2}$  producing a sustained high  $P_o$  in the physiological potential range.

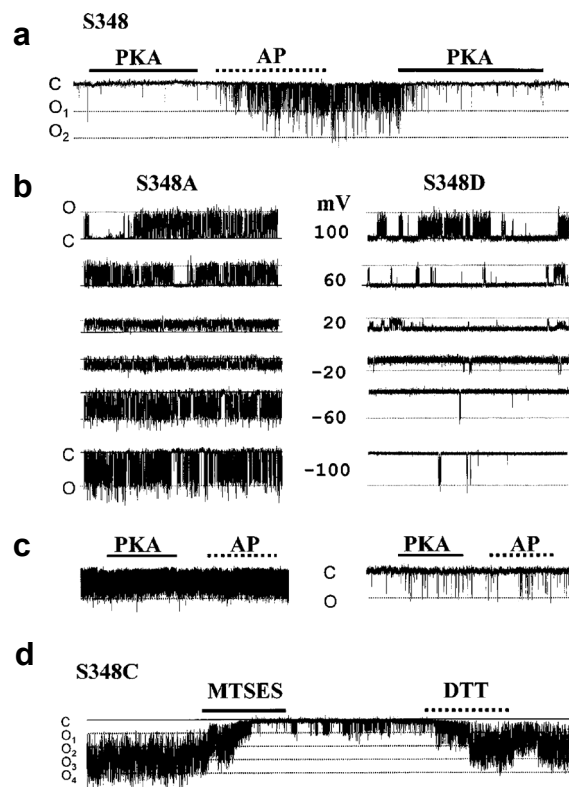


**Fig. 3.** KCNK2 channels have a voltage-dependent phenotype when residue 348 is negatively charged via phosphorylation, mutation or modification. Cloned KCNK2 channels were studied in inside-out mode with 100 mM symmetric KCl solution without  $MgCl_2$ . Channel state designations as in Fig. 1. Open levels have a step size of 6 pA at  $-60$  mV;  $O^*$  was not observed in the absence of magnesium.  $O_n$ , open level for that number of channels. (a) Wild-type cloned KCNK2 channels show decreased activity when treated with PKA and ATP (solid bar) and increased activity when treated with with AP (dashed bar). Shown at  $-60$  mV; trace duration, 7 min; sampled at 1 kHz, filtered at 200 Hz. (b) Mutation of KCNK2 serine 348 to alanine (S348A) or aspartate (S348D) recapitulates the effects of enzyme treatments. A single S348A KCNK2 channel (left) shows a uniform  $P_o$  from  $-100$  to  $100$  mV, whereas a single S348D KCNK2 channel (right) shows voltage dependence. Trace duration, 2 s; sampled at 20 kHz, filtered at 2 kHz. (c) Single KCNK2 channels mutated to alanine or aspartate at residue 348 are insensitive to PKA and ATP (solid bar) or AP (dashed bar); shown at  $-60$  mV. Trace duration, 5 min; sampled at 1 kHz, filtered at 200 Hz. (d) Application of  $10$  mM MTSES (solid bar) to four S348C KCNK2 channels held at  $-60$  mV reduces channel activity. Whereas washout did not reverse the effect, application of  $5$  mM dithiothreitol (DTT, dashed bar) restored function. Trace duration, 5 min; sampled at 1 kHz, filtered at 200 Hz.

### Other pathways also alter KCNK2 phenotype

Whereas phosphorylation of KCNK2 on serine 348 produces a voltage-dependent phenotype, it seems unlikely that the phosphate is a structural component of the channel gate (although it could be a source of gating charge). Two other manipulations that placed a negative charge on the residue yielded similar changes, that is, mutation to aspartate (Fig. 3b) and mutation to cysteine followed by MTSES modification (Fig. 3d). Moreover, KCNK2 channels remain subject to phenotypic regulation after ablation of the PKA consensus site at serine 348. In two of nine excised single-channel patches, S348A KCNK2 revealed an intermediate phenotype at baseline ( $P_{o100} = 0.4 \pm 0.2$ ,  $P_{o-100}/P_{o100} = 0.3 \pm 0.1$ ); in these cases, internal application of 1 mM ATP without PKA increased  $P_o$  and abolished voltage dependence ( $P_o = 0.7 \pm 0.2$ ,  $P_{o-100}/P_{o100} = 0.9 \pm 0.1$ ) in an AP-reversible fashion. This suggests that an endogenous kinase can act on the mutant channel (or an accessory protein) to alter KCNK2 phenotype. Furthermore, 10  $\mu$ M arachidonic acid, a regulator of whole-cell KCNK2 currents<sup>21</sup>, modified whole-cell S348D currents to resemble those of S348A: magnitude was increased and rectification was altered from outward toward open (data not shown). These findings (albeit with mutant channels) suggest other pathways may regulate KCNK2 in a manner reciprocal to that of PKA. Thus, the phenotypic change in KCNK2 described here follows channel phosphorylation, but its mechanistic basis remains to be discerned.

### A broader role for an emerging superfamily

Fifty years after the description of potassium-selective leak channels, their genes have been identified<sup>17</sup>. KCNK genes are numerous, have wide tissue distribution, and encode 2P/4TM subunits that form KCNK channels. Studies of cloned single KCNK0 channels have confirmed that leak accrues from channels open at rest<sup>40</sup> and have demonstrated that leak channels are not always open, but rather, are subject to strict regulation like their native counterparts<sup>25</sup>. Thus, the excitatory influence of neurotransmitter-mediated inhibition of KCNK3 in cortical and thalamic neurons seems key to 'state-switching' and, hence, transitions between sleep and wakefulness<sup>41-43</sup>. In contrast, the volatile anesthetic halothane activates KCNK3 in hypoglossal and locus coeruleus neurons hyper-polarizing the cells and decreasing spike activity and this is thought to mediate immobilization, as well as analgesic and hypnotic actions of the drug<sup>44</sup>. Thus, regulation of KCNK channels has been associated with more or less leak; this report demonstrates that the repertoire of these channels is more diverse.

KCNK channels that show function (KCNK0, 2, 3, 4, 5, 6, 9, 10, 13 and TWK18) all demonstrate attributes expected for potassium leak conductances: currents are present at rest and seem to rise instantly with voltage steps. Activity is voltage independent and permeation behavior follows expectations for open (Goldman-Hodgkin-Katz) rectification: both inward and outward single channel currents are large with symmetric potassium across the membrane. So KCNK0 (refs. 16, 40) and KCNK2 in the absence of magnesium (Fig. 4) show linear unitary current-voltage relationships, whereas KCNK2 in the presence of magnesium passes somewhat larger outward currents (Fig. 4b), and KCNK9 slightly larger inward currents<sup>45</sup>. Nonetheless, because current flows more easily from a side of high permeant ion concentration, and potassium inside an animal cell is higher than outside, all KCNK channels pass larger outward unitary currents under physiological conditions. These open channel attributes are not altered when KCNK2 channels transform from voltage independent to voltage gated.

Discordant descriptions of whole-cell KCNK2 currents can now be understood. Macroscopic currents like those we observed when serine 348 was altered to alanine (Fig. 4c) have been reported under some baseline conditions<sup>22,23</sup> and after exposure to chloroform<sup>19</sup> or lysophospholipids<sup>21</sup>; these demonstrate operation of KCNK2 as an open rectifier that is weakly blocked by external magnesium in a voltage-dependent fashion. Other treatments<sup>19-21</sup> yielded currents like those we observed after mutation of serine 348 to aspartate, and KCNK2 was voltage gated (Fig. 4c). These disparate phenotypes can be difficult to distinguish under physiological conditions because both produce large, positive outward currents (Fig. 4c). However, at voltages negative to 0 mV, the two behaviors are readily distinguished and are expected to have very different effects on excitability. Operating as an open rectifier, KCNK2 passes currents both above and below  $E_K$  ( $\sim -85$  mV), stabilizing the cell at rest (Fig. 4d). When voltage gated, KCNK2 only passes significant currents above threshold (Fig. 4d), because changes in open probability are half maximal above 0 mV (Fig. 4a), rise to threshold is unimpeded, and recovery and repetitive firing are facilitated.

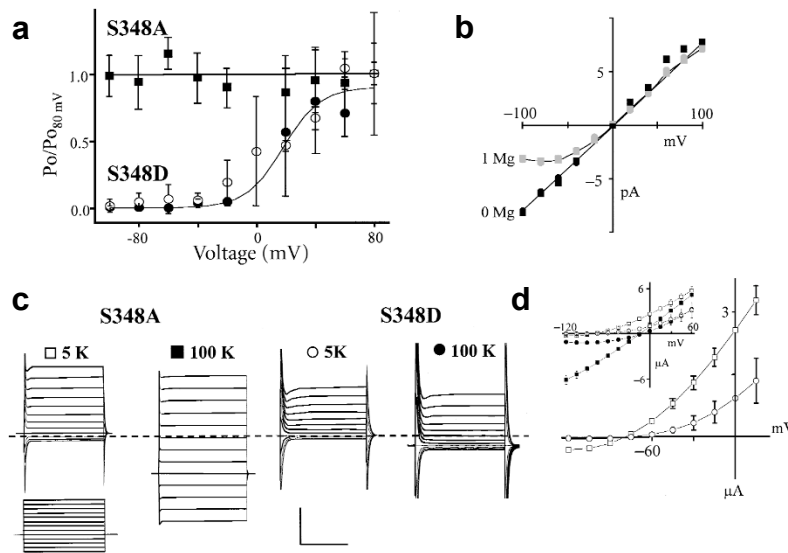


**Fig. 4.** Voltage-dependent activation of KCNK2 is not sensitive to potassium reversal potential or due to magnesium blockade. KCNK2 channels studied in inside-out patches or by two-electrode voltage clamp. (a) Normalized open probability–voltage relationships for cloned KCNK2 channels. S348A channels (solid squares) have a uniform  $P_o$ , whereas S348D channels (circles) are voltage dependent ( $n = 6–7$ ).  $V_{1/2}$  for S348D channels was determined by fitting to a Boltzmann function,  $A_1 - A_2 / (1 + \exp[V_{1/2} - V]/V_S)^{-1} + A_2$ , and was almost the same in symmetric 100 mM KCl (solid circles) and asymmetric conditions (open circles, 5 mM KCl in bath, 100 mM KCl in pipette,  $n = 6$ ). This plot excludes the two S348A single channel patches that were of mixed phenotype before application of ATP. No solutions included magnesium. (b) Magnesium similarly inhibits inward current through S348A (squares) and S348D (circles) single channels. The principle single channel current level was measured in the absence of magnesium (0 Mg, solid symbols) and with 1 mM  $MgCl_2$  (1 Mg, gray symbols; the latter state is  $O^*$ ). The voltage dependence of block was modeled by a simplification of the approach of Woodhull, as described previously<sup>18</sup>. The apparent electrical distance traversed by magnesium,  $\delta$ , was  $-0.31 \pm 0.04$  and  $-0.29 \pm 0.03$  for S348A and S348D channels, respectively. Half-block was seen with 1 mM  $MgCl_2$  at  $-87 \pm 4$  and  $-85 \pm 4$  mV for S348A and S348D channels, respectively. (c) KCNK2 whole-cell currents in physiological and high external potassium. Sample current families from oocytes expressing S348A or S348D channels bathed with 5 or 100 mM potassium solution. Scale bars, 2  $\mu A$  and 100 ms; protocol indicates 200-ms pulses from  $-60$  mV to voltages of  $-120$  to 60 mV in steps of 10 mV. Current–voltage relationships for groups of 9 cells expressing S348A channels (open squares) or S348D channels (open circles) in 5 mM potassium solution. Inset, current–voltage relationships for cells in 5 mM potassium, and for the same cells expressing S348A channels (filled squares) or S348D channels (filled circles) in 100 mM potassium solution. Error bars, s.e.m.

## METHODS

**Molecular biology.** To clone rat KCNK2, primers were designed by homology to human KCNK2 (AF004711) and a rat EST and used with a rat brain cDNA library (Clontech, Palo Alto, California) and RACE methodology; the primers for 3' extension were 5'-GGCGGCCCT-GACTTGCTGGATCC-3' and 5'-GCCTTGCTGGGAATTCCCCTCTTTGGTTTTCTACTGG-3'; reverse complement primers were used for the 5' reactions. Two clones were sequenced on both strands and deposited (AF325671). Reverse transcription and amplification were done with 5'-GGCGGCCCTGACTTGCTGGATCC-3' and 5'-GACAGCTCAGGA GCCTCCTCATGAGTGCGG-3' using an RT-PCR ONE STEP kit (Qia-gen, Valencia, California) after RNA was isolated from single 10-cm confluent culture dishes using an RNeasy Mini kit (Qiagen). Human KCNK2 was cloned<sup>18</sup>, mutated and transcribed with T7 RNA polymerase (Ambion, Austin, Texas), as described<sup>25</sup>.

The line, provided by S. Rivkees (Yale University) and previously described<sup>24</sup>, was produced from embryonic rat hippocampal cells by retroviral transduction with temperature-sensitive simian virus 40 large tumor antigen. Cells were passed at 33°C in DMEM with 10% FBS, 50 mg/l penicillin/streptomycin and 200 mg/l of geneticine in tissue culture dishes coated with poly-lysine. Differentiation was induced by increasing culture temperature to 38°C, reducing FBS to 1%, and adding 0.1 mg/ml sodium pyruvate, 2 mM glutamine, 10 ng/ml human basic fibroblast growth factor, and N2 supplement (GIBCO BRL, Rockwell, Maryland; provides 5



mg/l insulin, 100 mg/l transferrin, 20 nM progesterone, 0.1 mM putrescine and 30 nM sodium selenite). These conditions were applied for 2 to 4 days before reverse transcription or biophysical study.

**Electrophysiology.** Oocytes were isolated from *Xenopus laevis* frogs (Nasco, Atkinson, Wisconsin), defolliculated by collagenase treatment and injected the same day with 46 nl of cRNA containing 0.25 to 2 ng of KCNK2 cRNA. Whole-cell currents were measured 1–5 days after cRNA injection by two-electrode voltage clamp using an oocyte clamp (Warner, Hamden, Connecticut) and pCLAMP8 software (Axon Instruments, Foster City, California) with bath solution containing 100 mM KCl, 1 mM MgCl<sub>2</sub>, 0.3 mM CaCl<sub>2</sub>, 5 mM HEPES, pH 7.5. Data were sampled at 5 kHz and filtered at 1 kHz. Electrodes were fabricated from borosilicate tubes (Garner Glass, Claremont, California), contained 3 M KCl and had resistances of 0.2–1 MΩ. Recordings were made under constant perfusion at room temperature.

For patch clamp studies, data were sampled with an Axon 200B amplifier using pCLAMP8 software (Axon Instruments, Foster City, California) and stored on videotape. Data were digitized at 10 or 20 kHz and filtered at 2 or 4 kHz with a Gaussian software filter. Data were analyzed with TAC software (Bruyton, Seattle, Washington). Amplitude levels were obtained by all-points histograms. Bath and pipette solution contained 100 mM KCl, 1 mM EGTA, 5 mM HEPES, pH 7.5 unless otherwise stated. Bath and pipette solutions for recordings with rat hippocampal cells included 1 mM MgCl<sub>2</sub>. Neither AP nor PKA and ATP revealed silent channels in patches without channel activity from either native or experimental cells (n = 3). To identify native KCNK2 channels, recordings were taken in 5-s steps and 20-mV increments from 100 to –100 mV, with an interpulse interval of 6 s and a holding voltage of 0 mV. Ultra-pure KCl was purchased from Alfa Aesar, Ward Hill, Massachusetts. ATP (sodium salt) was used at 1 mM and dithiothreitol (DTT), at 5 mM; both were purchased from Sigma (St. Louis, Missouri). PKA catalytic subunit was purchased from Calbiochem (La Jolla, California). Alkaline phosphatase was purchased from New England Biolabs (Beverly, Massachusetts). Stock enzyme solutions were stored at –20°C (AP) or –80°C (PKA) at 500x and diluted to a final level of 20 U/ml with bath solution before use. We stored 2-sulfonatoethyl methanethiosulfonate (MTSES; Toronto Research Chemicals, Downsview, Ontario) as a solid at 4°C and dissolved it in bath solution before use.

## ACKNOWLEDGEMENTS

This work was supported by grants to S.A.N.G. from the National Institutes of Health. D.B. is supported by the Child Health Research Center (Yale University) and an award from the National Institute of Diabetes and Digestive and Kidney Diseases. We thank F. Sesti and R. Goldstein for discussions and advice during the course of this work.

RECEIVED 16 FEBRUARY; ACCEPTED 21 FEBRUARY 2001

1. Goldman, D. E. Potential, impedance, and rectification in membranes. *J. Gen. Physiol.* **27**, 37–60 (1943).
2. Hodgkin, A. L. & Katz, B. The effect of sodium ions on the electrical activity of the giant axon of the squid. *J. Physiol. (Lond.)* **108**, 37–77 (1949).
3. Hodgkin, A. L. & Huxley, A. F. A quantitative description of membrane current and its application to conduction and excitation in nerve. *J. Physiol. (Lond.)* **117**, 500–544 (1952).
4. Hille, B. Ionic selectivity of Na and K channels of nerve membranes. *Membranes* **3**, 255–323 (1975).
5. Adams, D. J., Smith, S. J. & Thompson, S. H. Ionic currents in molluscan soma. *Annu. Rev. Neurosci.* **3**, 141–167 (1980).
6. Schmidt, H. & Stampfli, R. The effect of tetraethylammonium chloride on single Ranvier's nodes. *Pflugers Arch. Gesamte Physiol. Menschen Tiere* **287**, 311–325 (1966).
7. Hille, B. Potassium channels in myelinated nerve. Selective permeability to small cations. *J. Gen. Physiol.* **61**, 669–686 (1973).
8. Baker, M., Bostock, H., Grafe, P. & Martius, P. Function and distribution of three types of rectifying channel in rat spinal root myelinated axons. *J. Physiol. (Lond.)* **383**, 45–67 (1987).

9. Chang, D. C. Is the K<sup>+</sup> permeability of the resting membrane controlled by the excitable K<sup>+</sup> channel? *Biophys. J.* **50**, 1095–1100 (1986).
10. Jones, S. W. On the resting potential of isolated frog sympathetic neurons. *Neuron* **3**, 153–161 (1989).
11. Backx, P. H. & Marban, E. Background potassium current active during the plateau of the action potential in guinea pig ventricular myocytes. *Circ. Res.* **72**, 890–900 (1993).
12. Siegelbaum, S. A., Camardo, J. S. & Kandel, E. R. Serotonin & cyclic AMP close single K<sup>+</sup> channels in Aplysia sensory neurones. *Nature* **299**, 413–417 (1982).
13. Shen, K. Z., North, R. A. & Surprenant, A. Potassium channels opened by noradrenaline and other transmitters in excised membrane patches of guinea-pig submucosal neurones. *J. Physiol. (Lond.)* **445**, 581–599 (1992).
14. Buckler, K. J. A novel oxygen-sensitive potassium current in rat carotid body type I cells. *J. Physiol. (Lond.)* **498**, 649–662 (1997).
15. Ketchum, K. A., Joiner, W. J., Sellers, A. J., Kaczmarek, L. K. & Goldstein, S. A. N. A new family of outwardly-rectifying potassium channel proteins with two pore domains in tandem. *Nature* **376**, 690–695 (1995).
16. Goldstein, S. A. N., Price, L. A., Rosenthal, D. N. & Pausch, M. H. ORK1, a potassium-selective leak channel with two pore domains cloned from *Drosophila melanogaster* by expression in *Saccharomyces cerevisiae*. *Proc. Natl. Acad. Sci. USA* **93**, 13256–13261 (1996).
17. Goldstein, S. A. N., Bockenhauer, D., O’Kelly, I. & Zilberberg, N. Potassium leak channels with 2 P domains. *Nat. Reviews Neurosci.* **2**, 175–184 (2001).
18. Goldstein, S. A. N., Wang, K. W., Ilan, N. & Pausch, M. Sequence and function of the two P domain potassium channels: implications of an emerging superfamily. *J. Molec. Med.* **76**, 13–20 (1998).
19. Patel, A. J. et al. A mammalian two pore domain mechano-gated S-like K<sup>+</sup> channel. *EMBO J.* **17**, 4283–4290 (1998).
20. Maingret, F. et al. TREK-1 is a heat-activated background K<sup>+</sup> channel. *EMBO J.* **19**, 2483–2491 (2000).
21. Maingret, F., Patel, A. J., Lesage, F., Lazdunski, M. & Honore, E. Lysophospholipids open the two-pore domain mechano-gated K<sup>+</sup> channels TREK-1 and TRAAK. *J. Biol. Chem.* **275**, 10128–10133 (2000).
22. Fink, M. et al. Cloning, functional expression and brain localization of a novel unconventional outward rectifier K<sup>+</sup> channel. *EMBO J.* **15**, 6854–6862 (1996).
23. Meadows, H. J. et al. Cloning, localisation and functional expression of the human orthologue of the TREK-1 potassium channel. *Eur. J. Physiol.* **439**, 714–722 (2000).
24. Eves, E. M. et al. Immortal rat hippocampal cell lines exhibit neuronal and glial lineages and neurotrophin gene expression. *Proc. Natl. Acad. Sci. USA* **89**, 4373–4377 (1992).
25. Zilberberg, N., Ilan, N., Gonzalez-Colaso, R. & Goldstein, S. A. N. Opening and closing of KCNK0 potassium leak channels is tightly-regulated. *J. Gen. Physiol.* **116**, 721–734 (2000).
26. Zhou, Y. et al. A dynamically regulated 14-3-3, Slob, and slowpoke potassium channel complex in *Drosophila* presynaptic nerve terminals. *Neuron* **22**, 809–818 (1999).
27. Vandenberg, C. A. Inward rectification of a potassium channel in cardiac ventricular cells depends on internal magnesium ions. *Proc. Natl. Acad. Sci. USA* **84**, 2560–2564 (1987).
28. Kubo, Y., Reuveny, E., Slesinger, P. A., Jan, Y. N. & Jan, L. Y. Primary structure and functional expression of a rat G-protein-coupled muscarinic potassium channel. *Nature* **364**, 802–806 (1993).
29. Lopatin, A. N., Makhina, E. N. & Nichols, C. G. Potassium channel block by cytoplasmic polyamines as the mechanism of intrinsic rectification. *Nature* **372**, 366–369 (1994).
30. Fakler, B. et al. Strong voltage-dependent inward-rectification of inward-rectifier K<sup>+</sup> channels is caused by intracellular spermine. *Cell* **80**, 149–154 (1995).

31. Ahmed, A. et al. A molecular target for viral killer toxin: TOK1 potassium channels. *Cell* **99**, 283–291 (1999).
32. Vergani, P., Miosga, T., Jarvis, S. M. & Blatt, M. R. Extracellular K<sup>+</sup> and Ba<sup>2+</sup> mediate voltage-dependent inactivation of the outward-rectifying K<sup>+</sup> channel encoded by the yeast gene TOK1. *FEBS Lett.* **405**, 337–344 (1997).
33. Vergani, P., Hamilton, D., Jarvis, S. & Blatt, M. R. Mutations in the pore regions of the yeast K<sup>+</sup> channel YKC1 affect gating by extracellular K<sup>+</sup>. *EMBO J.* **17**, 7190–7198 (1998).
34. Loukin, S. H. et al. Random mutagenesis reveals a region important for gating of the yeast K<sup>+</sup> channel Ykc1. *EMBO J.* **16**, 4817–4825 (1997).
35. Loukin, S. H. & Saimi, Y. K<sup>+</sup>-dependent composite gating of the yeast K<sup>+</sup> channel, Tok1. *Biophys. J.* **77**, 3060–3070 (1999).
36. Sigworth, F. J. Voltage gating of ion channels. *Q. Rev. Biophys.* **27**, 1–40 (1994).
37. Yellen, G. The moving parts of voltage-gated ion channels. *Q. Rev. Biophys.* **31**, 239–295 (1998).
38. Bean, B. P. Neurotransmitter inhibition of neuronal calcium currents by changes in channel voltage dependence. *Nature* **340**, 153–156 (1989).
39. Colecraft, H. M., Patil, P. G. & Yue, D. T. Differential occurrence of reluctant openings in G-protein-inhibited N- and P/Q-type calcium channels. *J. Gen. Physiol.* **115**, 175–192 (2000).
40. Ilan, N. & Goldstein, S. A. N. KCNK0: single, cloned potassium leak channels are multi-ion pores. *Biophys. J.* **80**, 241–254 (2001).
41. McCormick, D. A. & Bal, T. Sleep and arousal: thalamocortical mechanisms. *Annu. Rev. Neurosci.* **20**, 185–215 (1997).
42. Millar, J. A. et al. A functional role for the two-pore domain potassium channel TASK-1 in cerebellar granule neurons. *Proc. Natl. Acad. Sci. USA* **97**, 3614–3618 (2000).
43. Talley, E. M., Lei, Q. B., Sirois, J. E. & Bayliss, D. A. TASK-1, a two-pore domain K<sup>+</sup> channel, is modulated by multiple neurotransmitters in motoneurons. *Neuron* **25**, 399–410 (2000).
44. Sirois, J. E., Lei, Q., Talley, E. M., Lynch, C. III & Bayliss, D. A. The TASK-1 two-pore domain K<sup>+</sup> channel is a molecular substrate for neuronal effects of inhalation anesthetics. *J. Neurosci.* **20**, 6347–6354 (2000).
45. Kim, Y., Bang, H. & Kim, D. TASK-3, a new member of the tandem pore K<sup>+</sup> channel family. *J. Biol. Chem.* **275**, 9340–9347 (2000).
46. Colquhoun, D. & Sigworth, F. J. in *Single-Channel Recording* (eds. B. Sakmann & E. Neher) 483–588 (Plenum, New York, 1995).